Proceedings of the 31st Chinese Control Conference
July 25-27, 2012, Hefei, China

Active Disturbance Rejection Control for Permanent Magnet Linear Motor

Tao Hu, Wenchao Xue, Yi Huang
Key Laboratory of Systems and Control, Academy of Mathematics and Systems Science, Chinese Academy of Sciences, Beijing 100190, P.R.China
E-mail: httoe@yahoo.cn, xuewensuper1985@yahoo.com.cn, yhuang@amss.ac.cn

Abstract: In this paper, we design ADRC for PMLM and propose RESO to estimate the disturbances. The theoretical analysis and simulation show that RESO-based ADRC can guarantee high-precision of PMLM.

Key Words: PMLM, nonlinear disturbance, RESO, ADRC, closed-loop stability

1 INTRODUCTION

The permanent magnet linear motor(PMLM) has got many applications, especially involving high-speed and high-precision motion control. As a kind of linear motor, PMLM has many advantages comparing to rotating motor, such as the simplicity in mechanical structure and the high accuracy. However, since PMLM has no mechanical transimission, the model uncertainties and external disturbances would take effect on the magnettor straightly without any buffering and diminish the stability and precision of the system[1]. Therefore, reducing these effects is of importance to achieve high-speed and high-precision motion control.

There are already some researches on applying the active disturbance rejection contro(ADRC) [13, 14, 17] for PMLM. In [2–4], both simulations and experiments show that the dynamic performance and robustness of the ADRC control system are better than the PID control system. In [5, 6], the idea of ADRC is combined with the model identification to improve the performance. In [7, 8], ADRC is combined with the feedforward strategy and the stability of the closed-loop system is discussed for a simplified linear PMLM model. The above researches are mainly based on simulations and experiments. The theoretical research, especially the analysis considering the nonlinear effects such as friction and magnetic resistance which are natural in PMLM is little. In this paper, a novel ADRC design is proposed for PMLM servo system and the performance of the closed-loop system is analyzed considering the nonlinear effects in PMLM.

This paper is organized as follows. The model of PMLM is introduced in Section 2. In Section 3, an ADRC design based on the reduced-order extended state observer(RESO) is proposed. The closed-loop performance and the relationship between the tracking errors and the ADRC parameters are discussed in Section 4. Simulation results are shown in Section 5. Finally, some concluding remarks are given in Section 6.

2 MATHEMATICAL MODEL OF PMLM

The dynamics of PMLM can be expressed as follows [9, 10]:

$$\begin{aligned} M\ddot{x} + D\dot{x} + F_d &= K_f i \\ K_e\dot{x} + L\dot{i} + Ri &= u(t) \end{aligned} \tag{1}$$

Supported by the National Center for Mathematics and Interdisciplinary Sciences, CAS and NSFC60821091.

where x denotes the motor position, M, D, F_d denote the mass of the moving thrust block, viscosity constant and disturbance, respectively; $u(t), i, R, L$ denote the motor terminal voltage, armature current, armature resistance and armature inductance, respectively; K_f denotes an electrical-mechanical energy conversion constant; and K_e is the back electromotive force(EMF) voltage.

Usually, F_d is composed of three parts:

$$F_d = F_{load} + F_{ripple} + F_{fric}, \tag{2}$$

where $F_{load}, F_{ripple}, F_{fric}$ denote the load force, the ripple force arising from the magnetic structure of PMLM and the frictional force, respectively.

The load force is assumed to be bounded as follows:

$$|F_{load}(t)| \leq F_{lM}, \forall t > 0. \tag{3}$$

The ripple force can be viewed as a sinusoidal function of the motor position with a period of a, an amplitude of A_r and a phrase φ [9, 10]:

$$F_{ripple} = A_r \sin(ax + \varphi). \tag{4}$$

The frictional force may be modeled as a combination of Coulomb friction, viscous friction and stiction, which may be written as [10–12]:

$$F_{fric} = [F_c + (F_s - F_c)e^{-(\frac{\dot{x}}{s})^2} + F_v|\dot{x}|]sign(\dot{x}), \tag{5}$$

where F_c, F_s, F_v, s denote the Coulomb friction, the magnitude of stiction, the viscous friction parameter and the lubricant parameter which may be determined by empirical experiments, respectively.

All parameters above can be regarded as constants.

Since the electrical time constant is typically much smaller than the mechanical one, the delay due to the electrical transient response can be ignored. Thus ignoring the influence of inductance L, the mathematical model of the PMLM is then simplified as

$$\ddot{x} = -a_1\dot{x} - \bar{f}_d + b_0 u(t), \tag{6}$$

where $a_1 = \frac{1}{M}(D + \frac{K_f K_e}{R})$, $b_0 = \frac{K_f}{MR}$, $\bar{f}_d = \frac{F_d}{M}$.

3 RESO BASED ADRC FOR PMLM

The key in ADRC is to online estimate the total uncertainty, which lumps the internal uncertain dynamics and the

external disturbances, by the extended state observer(ESO) [15, 16], and to compensate it in the controller design. Next, we will design an ADRC which is based on the reduced-order extended state observer(RESO) [18] for PMLM.

Denote $x_1 = x$ and $x_2 = \dot{x}_1$, we obtain the state equations of the system (6):

$$\begin{cases} \dot{x}_1 = x_2 \\ \dot{x}_2 = -a_1 x_2 - \bar{f}_d + b_0 u \\ y = x_1 \end{cases} \tag{7}$$

Denote:

$$x_3 = -a_1 x_2 - \bar{f}_d, \tag{8}$$

where $\bar{f}_d = \bar{f}_0 + f_v x_2, f_0 = \frac{1}{M}[F_{load} + F_{ripple} + (F_c + (F_s - F_c)e^{-(\frac{\dot{x}}{s})^2})sign(\dot{x})], f_v = \frac{F_v}{M}$.

Regarding x_3 which lumps the disturbance and uncertain internal dynamic as the total disturbance of the system, we design the following RESO for PMLM:

$$\begin{aligned} \begin{bmatrix} \dot{\hat{v}}_2 \\ \dot{\hat{v}}_3 \end{bmatrix} &= \begin{bmatrix} -\beta_1 & 1 \\ -\beta_2 & 0 \end{bmatrix} \begin{bmatrix} \hat{v}_2 \\ \hat{v}_3 \end{bmatrix} + \begin{bmatrix} -\beta_1^2 + \beta_2 \\ -\beta_1 \beta_2 \end{bmatrix} x_1 + \begin{bmatrix} 1 \\ 0 \end{bmatrix} b_0 u \\ \begin{bmatrix} \hat{x}_2 \\ \hat{x}_3 \end{bmatrix} &= \begin{bmatrix} \hat{v}_2 \\ \hat{v}_3 \end{bmatrix} + \begin{bmatrix} \beta_1 \\ \beta_2 \end{bmatrix} x_1 \end{aligned} \tag{9}$$

where $\beta_1 = 2\omega, \beta_2 = \omega^2$ and ω is the parameter of RESO (9).

Design a linear ADRC based on RESO above as follows:

$$\begin{cases} u = \frac{u_0 - \hat{x}_3}{b_0} \\ u_0 = k_p(v - x_1) + k_d(\dot{v} - \hat{x}_2) + \ddot{v} \end{cases} \tag{10}$$

where $k_p = \omega_c^2, k_d = 2\omega_c$, $v, \dot{v}, \ddot{v}$ are the reference signal, the reference velocity signal and the reference accelerator signal, respectively, which are all continuously differentiable, and $v, \dot{v}$ are bounded.

In the next section we will analyze the stability of the closed-loop system (7)(9)(10) and the relationship between the tracking errors and the ADRC parameters ω, ω_c.

4 STABILITY ANALYSIS

As a start, we consider load force, viscous friction and ripple force. Thus $\bar{f}_d$ will be $f_d = f_0 + f_v x_2$, where $f_0 = \frac{1}{M}[F_{load} + F_{ripple}]$.

First, we put forward the assumption on the load force $F_{load}(t)$.

Assumption I: $F_{load}(t)$ satisfies

(i) $F_{load}(t)$ is piecewise continuous and possesses only discontinuity points of the first kind $\{t_i\}_{i=1}^{\infty}, t_{i-1} < t_i$, and $\delta_t = \inf_i \{t_i - t_{i-1}\} > 0$;

(ii) $|F_{load}(t)|$ is differentiable in $(t_{i-1}, t_i), i = 1, 2, \cdots$;

(iii) F_{load} is bounded, and $\dot{F}_{load}$ is bounded in (t_{i-1}, t_i):

$$\begin{aligned} &|F_{load}(t)| \le F_{lM} < \infty, t > 0; \\ &|\dot{F}_{load}(t)| \le D_1 < \infty, t \ne t_i (i = 1, 2, \cdots) \end{aligned} \tag{11}$$

Introduce the variable $x^* = \begin{bmatrix} x_1^* & x_2^* \end{bmatrix}^T$, which is the trajectory of the following reference system:

$$\begin{aligned} \dot{x}_1^* &= x_2^* \\ \dot{x}_2^* &= \ddot{v} - k_p(x_1^* - v) - k_d(x_2^* - \dot{v}) \end{aligned}$$

with the initial value $x_1^*(t_0) = x(t_0), x_2^*(t_0) = x_2(t_0)$. From (12), x_1^* and x_2^* are bounded when $k_p > 0$ and $k_d > 0$.

Define the tracking error $\tilde{x} = \begin{bmatrix} \tilde{x}_1 \\ \tilde{x}_2 \end{bmatrix} = \begin{bmatrix} x_1 - x_1^* \\ x_2 - x_2^* \end{bmatrix}$, and the estimation error of RESO $\hat{e} = \begin{bmatrix} \hat{e}_2 \\ \hat{e}_3 \end{bmatrix} = \begin{bmatrix} \hat{x}_2 - x_2 \\ \hat{x}_3 - x_3 \end{bmatrix}$, the performance of the closed-loop system can be presented by the following theorem.

Theorem 1 *Under Assumptions I, there exists $\omega^* > 1$ such that for $\forall \omega \ge \omega^*$,*

$$\|\tilde{x}\| \le T_1 \frac{\ln \omega}{\omega}, \ t \in [t_0, \infty) \tag{12}$$

$$\|\hat{e}(t)\| \le T_2 \frac{1}{\omega}, \ t \in [t_{i-1} + 2c_{22}\frac{\ln \omega}{\omega}, t_i) \tag{13}$$

where $c_{22} = 1 + \frac{\sqrt{2}}{2}$, T_1 and T_2 are constants determined by ω_c, the range of initial value and the bounds of disturbances and the reference signal.

Proof of Theorem 1. The proof can be achieved by the following two steps.

Step 1: $x_1, x_2, \hat{e}_2, \hat{e}_3$ are bounded in $[t_0, \infty)$.

Introduce the transformation

$$\xi = \begin{bmatrix} \xi_2 \\ \xi_3 \end{bmatrix} = \begin{bmatrix} \omega \hat{e}_2 \\ \hat{e}_3 - f_0 \end{bmatrix}. \tag{14}$$

From (7), (9), (10), (12) and (14), we can have the closed-loop system:

$$\begin{bmatrix} \dot{\tilde{x}}_1 \\ \dot{\tilde{x}}_2 \\ \dot{\xi}_2 \\ \dot{\xi}_3 \end{bmatrix} = \begin{bmatrix} 0 & 1 & 0 & 0 \\ -\omega_c^2 & -2\omega_c & -2\omega_c/\omega & -1 \\ 0 & 0 & -2\omega & \omega \\ 0 & 0 & -\omega & 0 \end{bmatrix} \begin{bmatrix} \tilde{x}_1 \\ \tilde{x}_2 \\ \xi_2 \\ \xi_3 \end{bmatrix} + \begin{bmatrix} 0 \\ -f_0 \\ \omega f_0 \\ \eta_1 \end{bmatrix} \tag{15}$$

where $\eta_1 = -(\omega_c^2 \tilde{x}_1 + 2\omega_c \tilde{x}_2 + \frac{2\omega_c}{\omega}\xi_2 + \xi_3 + f_0)\tilde{a}_1 + (\omega_c^2 v + 2\omega_c \dot{v} + \ddot{v} - \omega_c^2 x_1^* - 2\omega_c x_2^*)\tilde{a}_1$, $\tilde{a}_1 = a_1 + f_v$.

Denote

$$A_c = \begin{bmatrix} 0 & 1 \\ -\omega_c^2 & -2\omega_c \end{bmatrix}, B_c = \begin{bmatrix} 0 & 0 \\ -2\omega_c/\omega & -1 \end{bmatrix}, A_\xi = \begin{bmatrix} -2 & 1 \\ -1 & 0 \end{bmatrix}.$$

Since A_c, A_ξ are Hurwitz, there exist positive definite matrices P_1 and P_2 satisfying

$$A_c^T P_1 + P_1 A_c = -I_2, \ c_{11} I_2 \le P_1 \le c_{12} I_2 \tag{16}$$

$$A_\xi^T P_2 + P_2 A_\xi = -I_2, \ c_{21} I_2 \le P_2 \le c_{22} I_2 \tag{17}$$

where c_{11}, c_{12} are the minimum and maximum eigenvalue of P_1, respectively; c_{21}, c_{22} are the minimum and maximum eigenvalue of P_2, respectively. According to (16)(17), we can get

$$\begin{aligned} P_1 &= \begin{bmatrix} \frac{\omega_c^2 + 5}{4\omega_c} & \frac{1}{2\omega_c^2} \\ \frac{1}{2\omega_c^2} & \frac{\omega_c^2 + 1}{4\omega_c^3} \end{bmatrix}, \ P_2 = \begin{bmatrix} \frac{1}{2} & -\frac{1}{2} \\ -\frac{1}{2} & \frac{3}{2} \end{bmatrix} \\ c_{11} &= \frac{1}{8\omega_c^3}[\omega_c^4 + 6\omega_c^2 + 1 - \sqrt{(\omega_c^4 + 6\omega_c^2 + 1)(\omega_c^4 + 2\omega_c^2 + 1)}] \\ c_{12} &= \frac{1}{8\omega_c^3}[\omega_c^4 + 6\omega_c^2 + 1 + \sqrt{(\omega_c^4 + 6\omega_c^2 + 1)(\omega_c^4 + 2\omega_c^2 + 1)}] \\ c_{21} &= \frac{2 - \sqrt{2}}{2}, \ c_{22} = \frac{2 + \sqrt{2}}{2} \end{aligned} \tag{18}$$

All vector norms and matrix norms in the proof below are 2-norms except being pointed out specially.

Define $V_1(\tilde{x}) = \tilde{x}^T P_1 \tilde{x}$. Along the trajectory of (15),

$$\dot{V}_1(\tilde{x}) = 2\tilde{x}^T P_1 \dot{\tilde{x}} = -\|\tilde{x}\|^2 + 2\tilde{x}^T P_1 (B_c \xi - \begin{bmatrix} 0 & 1 \end{bmatrix}^T f_0)$$

When $\omega \geq 2\omega_c$,

$$\begin{aligned} \|P_1 B_c\| \leq \sqrt{2}\|P_1 B_c\|_1 &= \sqrt{2}\| \begin{bmatrix} -2n\omega_c/\omega & -n \\ -2l\omega_c/\omega & -l \end{bmatrix} \|_1 \\ &= \sqrt{2}(n+l)max\{2\omega_c/\omega, 1\} \\ &= \sqrt{2}(\frac{1}{2\omega_c^2} + \frac{\omega_c^2+1}{4\omega_c^3}) \end{aligned}$$

$$\begin{aligned} \|P_1 \begin{bmatrix} 0 & 1 \end{bmatrix}^T f_0\| &= |f_0|\sqrt{n^2+l^2} \\ &= |f_0|\sqrt{(\frac{1}{2\omega_c^2})^2 + (\frac{\omega_c^2+1}{4\omega_c^3})^2} \end{aligned} \tag{19}$$

Since $f_0 = \frac{1}{M}(F_{load} + F_{ripple})$, $|f_0|$ is bounded. Denote

$$|f_0| \leq \kappa_1,\ \kappa_1 = \frac{F_{lm} + A_r}{M}. \tag{20}$$

Define

$$r_1(\omega_c) = 2\sqrt{2}(\frac{1}{2\omega_c^2} + \frac{\omega_c^2+1}{4\omega_c^3}), \tag{21}$$

$$r_2(\omega_c) = 2\sqrt{(\frac{1}{2\omega_c^2})^2 + (\frac{\omega_c^2+1}{4\omega_c^3})^2}, \tag{22}$$

then

$$\dot{V}_1(\tilde{x}) \leq -\|\tilde{x}\|^2 + r_1(\omega_c)\|\tilde{x}\| \cdot \|\xi\| + \kappa_1 r_2(\omega_c)\|\tilde{x}\|. \tag{23}$$

Define $V_2(\xi) = \xi^T P_2 \xi$, $K_1 = \begin{bmatrix} \omega_c^2 & 2\omega_c \end{bmatrix}$, $K_2 = \begin{bmatrix} 2\omega_c/\omega & 1 \end{bmatrix}$. Along the trajectory of (15),

$$\begin{aligned} \dot{V}_2(\xi) =& 2\xi^T P_2(\omega A_\xi \xi + \begin{bmatrix} \omega f_0 \eta_2 \end{bmatrix}^T) \\ =& -\omega\|\xi\|^2 + 2\xi^T P_2[\omega \begin{bmatrix} 1 & 0 \end{bmatrix}^T f_0 + \begin{bmatrix} 0 & 1 \end{bmatrix}^T (-K_1\tilde{x} \\ & - K_2\xi - f_0 + \omega_c^2 v + 2\omega_c \dot{v} + \ddot{v} - \omega_c^2 x_1^* - 2\omega_c x_2^*)\tilde{a}_1]. \end{aligned}$$

Suppose $|f_0 - (\omega_c^2 v + 2\omega_c \dot{v} + \ddot{v} - \omega_c^2 x_1^* - 2\omega_c x_2^*)| \leq \kappa_2$, and define

$$\begin{aligned} s_1(\omega_c) &= |\tilde{a}_1|\sqrt{10((2\omega_c)^2 + \omega_c^4)}, \\ s_2 &= 2\sqrt{5} \cdot |\tilde{a}_1|, \\ s_3 &= \kappa_2\sqrt{10} \cdot |\tilde{a}_1|. \end{aligned} \tag{24}$$

When $\omega \geq 2\omega_c$,

$$\|P_2 \begin{bmatrix} 0 & 1 \end{bmatrix}^T K_1\| \leq \frac{s_1(\omega_c)}{2|\tilde{a}_1|},\ \|P_2 \begin{bmatrix} 0 & 1 \end{bmatrix}^T K_2\| \leq \frac{s_2}{2|\tilde{a}_1|},$$

$$\|P_2 \begin{bmatrix} 0 & 1 \end{bmatrix}^T (f_0 - (\omega_c^2 v + 2\omega_c \dot{v} + \ddot{v} - \omega_c^2 x_1^* - 2\omega_c x_2^*))\| \leq \frac{s_3}{2|\tilde{a}_1|}.$$

Thus

$$\begin{aligned} \dot{V}_2(\xi) \leq& -(\omega - s_2)\|\xi\|^2 + (\sqrt{2}\omega\kappa_1 + s_3)\|\xi\| \\ & + s_1(\omega_c)\|\tilde{x}\| \cdot \|\xi\|. \end{aligned}$$

Define

$$\rho_1 = 2\sqrt{c_{12}}[\frac{\rho_2}{\sqrt{c_{21}}} r_1(\omega_c) + \kappa_1 r_2(\omega_c)], \tag{25}$$

$$\rho_2 = max\{\sqrt{V_2(\xi(t_0))},\ (\sqrt{2}+1)\sqrt{c_{22}}\kappa_1\}, \tag{26}$$

We can come to the conclusion that when $\omega > \frac{1}{\kappa_1}(\frac{\rho_1}{\sqrt{c_{11}}} s_1(\omega_c) + \frac{\rho_2}{\sqrt{c_{22}}} s_2 + s_3)$, $\Omega = \{(\tilde{x}, \xi) | \sqrt{V_1(\tilde{x})} \leq \rho_1,\ \sqrt{V_2(\xi)} \leq \rho_2\}$ is a positively invariant set of the trajectory of (15) for $t \in [t_0, \infty)$ by the following discussion.

i)If $\sqrt{V_1(\tilde{x})} = \rho_1$ and $\sqrt{V_2(\xi)} \leq \rho_2$, according to (23), along the trajectory of (15),

$$\begin{aligned} \dot{V}_1(\tilde{x}) &\leq -\|\tilde{x}\| \cdot [\|\tilde{x}\| - (r_1(\omega_c)\|\xi\| + \kappa_1 r_2(\omega_c))] \\ &\leq -\|\tilde{x}\| \cdot [\frac{\rho_1}{\sqrt{c_{12}}} - (r_1(\omega_c)\frac{\rho_2}{\sqrt{c_{21}}} + \kappa_1 r_2(\omega_c))] \\ &\leq -\|\tilde{x}\| \cdot [r_1(\omega_c)\frac{\rho_2}{\sqrt{c_{21}}} + \kappa_1 r_2(\omega_c)] \leq 0 \end{aligned} \tag{27}$$

ii)If $\sqrt{V_1(\tilde{x})} \leq \rho_1$ and $\sqrt{V_2(\xi)} = \rho_2$, according to (25), along the trajectory of (15)

$$\begin{aligned} \dot{V}_2(\xi) &\leq -\|\xi\| \cdot [(\omega - s_2)\|\xi\| - ((\sqrt{2}\omega\kappa_1 + s_3) + s_1(\omega_c)\|\tilde{x}\|)] \\ &\leq -\|\xi\| \cdot [(\omega - s_2)\frac{\rho_2}{\sqrt{c_{22}}} - ((\sqrt{2}\omega\kappa_1 + s_3) + s_1(\omega_c)\frac{\rho_1}{\sqrt{c_{11}}})] \\ &\leq -\|\xi\| \cdot [(\frac{\rho_2}{\sqrt{c_{22}}} - \sqrt{2}\kappa_1)\omega - (\frac{\rho_2}{\sqrt{c_{22}}} s_2 + s_3 + s_1(\omega_c)\frac{\rho_1}{\sqrt{c_{11}}})] \\ &\leq -\|\xi\| \cdot [\kappa_1\omega - (\frac{\rho_2}{\sqrt{c_{22}}} s_2 + s_3 + s_1(\omega_c)\frac{\rho_1}{\sqrt{c_{11}}})] < 0 \end{aligned} \tag{28}$$

From the analysis above, we can draw the conclusion that if ADRC parameters ω and ω_c satisfy

$$\omega > max\{2\omega_c,\ \frac{1}{\kappa_1}(\frac{\rho_1}{\sqrt{c_{11}}} s_1(\omega_c) + \frac{\rho_2}{\sqrt{c_{22}}} s_2 + s_3)\}, \tag{29}$$

then $\|\tilde{x}\|$, $\|\xi\|$ are bounded,

$$\|\tilde{x}\| \leq \frac{\rho_1}{\sqrt{c_{11}}},\ \|\xi\| \leq \frac{\rho_2}{\sqrt{c_{21}}}. \tag{30}$$

Since $\tilde{x} = \begin{bmatrix} x_1 - x^* \\ x_2 - \dot{x}^* \end{bmatrix}$, x_1, x_2 are bounded. And from (14), $\hat{e}_2$, $\hat{e}_3$ are bounded.

Step 2: Since $f_0 = \frac{1}{M}(F_{load} + F_{ripple})$, the discontinuity points of f_0 are the same as those of $F_{load}(t)$. Define the generalized derivative of f_0 as:

$$\dot{f}_0 = \begin{cases} \frac{df_0}{dt}, & t \neq t_i \\ H_i\delta(t - t_i), & t = t_i \end{cases} \tag{31}$$

where $|\frac{df_0}{dt}| \leq D_2 < \infty$, $|H_i| \leq H < \infty$, and $\delta(\cdot)$ has the property as follows:

$$\int \delta(t - t_i)dt = \begin{cases} 0, & t < t_i \\ 1, & t \geq t_i \end{cases}$$

Introduce a new transformation

$$\bar{\xi} = \begin{bmatrix} \bar{\xi}_2 \\ \bar{\xi}_3 \end{bmatrix} = \begin{bmatrix} \omega\hat{e}_2 \\ \hat{e}_3 \end{bmatrix}. \tag{32}$$

From (7)(9)(10)(12)(32), we have

$$\begin{bmatrix} \dot{\tilde{x}}_1 \\ \dot{\tilde{x}}_2 \\ \dot{\bar{\xi}}_2 \\ \dot{\bar{\xi}}_3 \end{bmatrix} = \begin{bmatrix} 0 & 1 & 0 & 0 \\ -\omega_c^2 & -2\omega_c & -2\omega_c/\omega & -1 \\ 0 & 0 & -2\omega & \omega \\ 0 & 0 & -\omega & 0 \end{bmatrix} \begin{bmatrix} \tilde{x}_1 \\ \tilde{x}_2 \\ \bar{\xi}_2 \\ \bar{\xi}_3 \end{bmatrix} + \begin{bmatrix} 0 \\ 0 \\ 0 \\ \eta_2 \end{bmatrix} \tag{33}$$

where

$$\begin{aligned}\eta_2 =& -(\omega_c^2\tilde{x}_1 + 2\omega_c\tilde{x}_2 + 2\frac{\omega_c}{\omega}\bar{\xi}_2 + \bar{\xi}_3)\tilde{a}_1 \\ &+ (\omega_c^2 v + 2\omega_c\dot{v} + \ddot{v} - \omega_c^2 x_1^* - 2\omega_c x_2^*)\tilde{a}_1 + \dot{f}_0.\end{aligned}$$

Compare the transformations (14) and (32), we have

$$\begin{aligned}\|\bar{\xi}\| =& \sqrt{\bar{\xi}_2^2 + \bar{\xi}_3^2} = \sqrt{\xi_2^2 + (\xi_3 + f_0)^2} \\ \le& \sqrt{2}\cdot\sqrt{\xi_2^2 + \xi_3^2 + f_0^2} \\ \le& \sqrt{2}(\|\xi\| + |f_0|)\end{aligned} \tag{34}$$

Since $\|\xi\| \le \frac{\rho_2}{\sqrt{c_{21}}}$ and $|f_0| \le \kappa_1$, $\bar{\xi}$ is also bounded. Denote

$$\|\bar{\xi}\| \le \rho_3,\ \rho_3 = \sqrt{2}(\frac{\rho_2}{\sqrt{c_{21}}} + \kappa_1). \tag{35}$$

When $t_0 \le t < t_1$, along the trajectory of (33), there is

$$\dot{V}_2(\bar{\xi}) = 2\bar{\xi}^T P_2(\omega A_\xi \bar{\xi} + \begin{bmatrix}0 & 1\end{bmatrix}^T \eta_2).$$

From (34), η_2 is bounded at all continuous points of f_0, denote $\|\eta_2(t)\| \le \kappa_3, t \ne t_i, i = 1, 2, \cdots$, where $\kappa_3 = \kappa_3(\omega_c, \rho_1, \rho_2, v, \dot{v}, \ddot{v}, A_r, D_1)$, that is κ_3 is a constant related with ω_c, the range of initial value and the bounds of disturbances and the reference signal.

Denote $s_4 = \sqrt{10}\kappa_3$, then

$$\|P_2\begin{bmatrix}0 & 1\end{bmatrix}^T\|\|\eta_2| = \frac{\sqrt{10}}{2}|\eta_2| \le \frac{\sqrt{10}}{2}\kappa_3 = \frac{s_4}{2}. \tag{36}$$

Thus $\dot{V}_2(\bar{\xi}) \le -\omega\|\bar{\xi}\|^2 + s_4\|\bar{\xi}\|$, and

$$\begin{aligned}\frac{d}{dt}\sqrt{V_2(\bar{\xi})} = \frac{\dot{V}_2(\bar{\xi})}{2\sqrt{V_2(\bar{\xi})}} &\le -\omega\frac{\|\bar{\xi}\|^2}{2\sqrt{V_2(\bar{\xi})}} + \frac{s_4\|\bar{\xi}\|}{2\sqrt{V_2(\bar{\xi})}} \\ &\le -\omega\frac{\sqrt{V_2(\bar{\xi})}}{2c_{22}} + \frac{s_4}{2\sqrt{c_{21}}}.\end{aligned} \tag{37}$$

According to the Gronwall-Bellman inequality, when $t_0 \le t < t_1$, there is

$$\begin{aligned}\sqrt{V_2(\bar{\xi})} &\le \frac{1}{\omega}\frac{c_{22}s_4}{\sqrt{c_{21}}} + \sqrt{V_2(\bar{\xi}(t_0))}e^{-\frac{\omega}{2c_{22}}(t-t_0)} \\ &\le \frac{1}{\omega}\frac{c_{22}s_4}{\sqrt{c_{21}}} + \sqrt{c_{22}}\|\xi(t_0)\|e^{-\frac{\omega}{2c_{22}}(t-t_0)} \\ &\le \frac{1}{\omega}\frac{c_{22}s_4}{\sqrt{c_{21}}} + \omega\rho_3\sqrt{c_{22}}e^{-\frac{\omega}{2c_{22}}(t-t_0)}\end{aligned} \tag{38}$$

If $\delta_t = \inf_i\{t_i - t_{i-1}\} \le \frac{2c_{22}}{e}$, $\{\omega|\delta_t = \frac{2c_{22}ln\omega}{\omega}\} \ne \emptyset$. Denote

$$\omega_1 = \begin{cases} max\{\omega|\delta_t = \frac{2c_{22}ln\omega}{\omega}\}, & \delta_t \le \frac{2c_{22}}{e} \\ 0, & \delta_t > \frac{2c_{22}}{e}\end{cases} \tag{39}$$

then when $\omega > \omega_1$, there is

$$\frac{2c_{22}\ln\omega}{\omega} < \delta_t. \tag{40}$$

Define $t_0^* = t_0 + \frac{4c_{22}\ln\omega}{\omega}$, then from (40) $t_0^* < t_1$, and

$$e^{-\frac{\omega}{2c_{22}}(t-t_0)} \le \frac{1}{\omega},\ t \ge t_0^* \tag{41}$$

From (38)(41),

$$\sqrt{V_2(\bar{\xi})} \le \frac{1}{\omega}(\frac{c_{22}}{\sqrt{c_{21}}}s_4 + \rho_3\sqrt{c_{22}}),\ t \in [t_0^*, t_1) \tag{42}$$

Thus

$$\|\bar{\xi}\| \le \frac{1}{\omega}(\frac{c_{22}}{c_{21}}s_4 + \frac{\sqrt{c_{22}}}{\sqrt{c_{21}}}\rho_3),\ t \in [t_0^*, t_1) \tag{43}$$

From the transformation (32), we can get

$$\|\hat{e}\| \le \|\bar{\xi}\| \le \frac{1}{\omega}(\frac{c_{22}}{c_{21}}s_4 + \frac{\sqrt{c_{22}}}{\sqrt{c_{21}}}\rho_3),\ t \in [t_0^*, t_1) \tag{44}$$

Similarly, we can prove that for $i \ge 1$,

$$\|\hat{e}\| \le \frac{1}{\omega}(\frac{c_{22}}{c_{21}}s_4 + \frac{\sqrt{c_{22}}}{\sqrt{c_{21}}}\rho_3),\ t \in [t_i^*, t_{i+1}) \tag{45}$$

where $t_i^* = t_i + \frac{2c_{22}\ln\omega}{\omega} < t_{i+1}$.

Next, we will prove $\|x(t) - x^*(t)\| \le O(\frac{\ln\omega}{\omega}),\ t \in [t_0, \infty)$.

Along the trajectory of (33),

$$\dot{V}_1(\tilde{x}) = 2\tilde{x}^T P_1\dot{\tilde{x}} \le -\|\tilde{x}\|^2 + r_1(\omega_c)\|\bar{\xi}\|\cdot\|\tilde{x}\|.$$

Thus

$$\begin{aligned}\frac{d}{dt}\sqrt{V_1(\tilde{x})} = \frac{\dot{V}_1(\tilde{x})}{2\sqrt{V_1(\tilde{x})}} &\le -\frac{\|\tilde{x}\|^2}{2\sqrt{V_1(\tilde{x})}} + \frac{r_1(\omega_c)\|\tilde{x}\|\cdot\|\bar{\xi}\|}{2\sqrt{V_1(\tilde{x})}} \\ &\le -\frac{\sqrt{V_1(\tilde{x})}}{2c_{12}} + \frac{r_1(\omega_c)\|\bar{\xi}\|}{2\sqrt{c_{11}}}.\end{aligned}$$

According to the Gronwall-Bellman inequality and because of $\tilde{x}(t_0) = 0$,

$$\sqrt{V_1(\tilde{x})} \le \frac{r_1(\omega_c)}{2\sqrt{c_{11}}}\int_{t_0}^{t} e^{-\frac{t-\tau}{2c_{12}}}\|\bar{\xi}(\tau)\|d\tau. \tag{46}$$

When $t_{k-1} \le t < t_k$,

$$\begin{aligned}\sqrt{V_1(\tilde{x})} \le& \frac{r_1(\omega_c)}{2\sqrt{c_{11}}}(\sum_{i=1}^{k}\int_{t_{i-1}}^{t_{i-1}^*} e^{-\frac{t-\tau}{2c_{12}}}\|\bar{\xi}(\tau)\|d\tau \\ &+ \sum_{i=1}^{k-1}\int_{t_{i-1}^*}^{t_i} e^{-\frac{t-\tau}{2c_{12}}}\|\bar{\xi}(\tau)\|d\tau + \int_{t_{k-1}^*}^{t} e^{-\frac{t-\tau}{2c_{12}}}\|\bar{\xi}(\tau)\|d\tau)\end{aligned}$$

Since $\|\bar{\xi}\| \le \rho_3$,

$$\begin{aligned}&\sum_{i=1}^{k-1}\int_{t_{i-1}^*}^{t_i} e^{-\frac{t-\tau}{2c_{12}}}\|\bar{\xi}(\tau)\|d\tau + \int_{t_{k-1}^*}^{t} e^{-\frac{t-\tau}{2c_{12}}}\|\bar{\xi}(\tau)\|d\tau \\ &< (\frac{c_{22}}{c_{21}}s_4 + \frac{\sqrt{c_{22}}}{\sqrt{c_{21}}}H)\frac{1}{\omega},\end{aligned} \tag{47}$$

$$\begin{aligned}&\sum_{i=1}^{k}\int_{t_{i-1}}^{t_{i-1}^*} e^{-\frac{t-\tau}{2c_{12}}}\|\bar{\xi}(\tau)\|d\tau \le 4c_{22}\rho_4\frac{\ln\omega}{\omega}\sum_{i=1}^{k} e^{-\frac{t-t_i}{2c_{12}}} \\ &\le 4c_{22}\rho_4\frac{e^{\frac{\triangle_t}{2c_{12}}}}{1 - e^{-\frac{\triangle_t}{2c_{12}}}}\frac{\ln\omega}{\omega}.\end{aligned} \tag{48}$$

From (47)(48), we can have

$$\sqrt{V_1(\tilde{x})} \le \frac{r_1(\omega_c)}{2\sqrt{c_{11}}}[(\frac{c_{22}}{c_{21}}s_4 + \frac{\sqrt{c_{22}}}{\sqrt{c_{21}}}H)\frac{1}{\omega} + \frac{4c_{22}\rho_3 e^{\frac{\triangle_t}{2c_{12}}}}{1 - e^{-\frac{\triangle_t}{2c_{12}}}}\frac{\ln\omega}{\omega}].$$

Thus

$$\|\tilde{x}\| \leq \frac{r_1(\omega_c)}{2\sqrt{c_{11}}}[(\frac{c_{22}}{c_{21}}s_4 + \frac{\sqrt{c_{22}}}{\sqrt{c_{21}}}H)\frac{1}{\omega} + \frac{4c_{22}\rho_3 e^{\frac{\triangle_t}{2c_{12}}}}{1-e^{-\frac{\triangle_t}{2c_{12}}}}\frac{\ln\omega}{\omega}]. \quad (49)$$

When $(\frac{c_{22}}{c_{21}}s_4 + \frac{\sqrt{c_{22}}}{\sqrt{c_{21}}}H)\frac{1}{\omega} \leq \frac{4c_{22}\rho_3 e^{\frac{\delta_t}{2c_{12}}}}{1-e^{-\frac{\delta_t}{2c_{12}}}}\frac{\ln\omega}{\omega}$, that is,

$$\omega \geq \omega_2 = e^{\frac{\frac{c_{22}}{c_{21}}s_4+\frac{\sqrt{c_{22}}}{\sqrt{c_{21}}}H}{4c_{22}\rho_3}\cdot\frac{e^{\frac{\delta_t}{2c_{12}}}-1}{e^{\frac{\delta_t}{c_{12}}}}}, \quad (50)$$

there is

$$\|\tilde{x}\| \leq \frac{4c_{22}\rho_3 r_1(\omega_c)}{c_{11}}\cdot\frac{e^{\frac{\delta_t}{c_{12}}}}{e^{\frac{\delta_t}{2c_{12}}}-1}\cdot\frac{\ln\omega}{\omega}. \quad (51)$$

Denote $\omega^* = max\{2\omega_c, \frac{1}{\kappa_1}(\frac{\rho_1}{\sqrt{c_{11}}}s_1(\omega_c) + \frac{\rho_2}{\sqrt{c_{22}}}s_2 + s_3), \omega_1, \omega_2\}$, from (45)(51), we can come to the conclusion that when $\omega \geq \omega^*$,

$$\|\tilde{x}\| \leq T_1\cdot\frac{\ln\omega}{\omega},\ t\in[t_0,\infty) \quad (52)$$

$$\|\hat{e}(t)\| \leq T_2\cdot\frac{1}{\omega},\ t\in[t_{i-1}+2c_{22}\frac{\ln\omega}{\omega}, t_i) \quad (53)$$

where

$$T_1 = \frac{4c_{22}\rho_3 r_1(\omega_c)}{c_{11}}\cdot\frac{e^{\frac{\delta_t}{c_{12}}}}{e^{\frac{\delta_t}{2c_{12}}}-1},$$

$$T_2 = \frac{c_{22}}{c_{21}}s_4 + \frac{\sqrt{c_{22}}}{\sqrt{c_{21}}}\rho_3.$$

are constants which are related with ω_c, the range of initial value and the bounds of disturbances and the reference signal.

Remark 1 (53) shows that $\hat{x}_2$ and $\hat{x}_3$ can estimate x_2 and x_3. The estimation error of the total disturbance is small except for the small regions around the discontinuous points and the precision of the estimation can be tuned by ω.

Remark 2 (52) shows that the larger ω is, the smaller the tracking error between $x(t)$ and $x^*(t)$ will be. And from (12), the larger ω_c is, the smaller the tracking errors between $x_1^*(t)$, $x_2^*(t)$ and v, $\dot{v}$ will be. Thus ω and ω_c can be tuned to guarantee the tracking precision.

5 SIMULATION

In this section, the application of RESO-based ADRC for PMLM is simulated. The simulation is carried out using Matlab/Simulink and the simulation step is 0.001s.

The reference signal in simulation is sine signal with amplitude 100mm and frequency $1rad/sec$. The load force is chosen as square wave with period 3s which is showd in Fig.1. Parameters of PMLM are shown in Table 1. In the simulation, the ADRC parameters are ω_c=500 and ω =1000, which are tuned according to the analysis discussed in section 4.

The reference signal and the system output are shown in Fig.2, while the tracking error is in Fig.3. Fig.2 and Fig.3 show that ADRC can achieve high precision.The performance of RESO is shown in Fig.4-7. Fig.4 and Fig.5 show

Table 1: Values of parameters

Parameter	Unit(SI)	Value
M	Kg	5.4
D	$N/(m\cdot s^{-1})$	10
R	Ohm	16.8
L	Henry	17.4×10^{-3}
K_f	N/A	130
K_e	$V/(m\cdot s^{-1})$	123
F_c	Newton	10
F_s	Newton	20
F_v	Newton	10
A_r	Newton	8.5
a	Rad/m	314
φ	-	0.05π
F_{lm}	Newton	100
x_s	$m\cdot s^{-1}$	0.1

the estimation performance of $\hat{x}_2$ for x_2 and the estimation error respectively, which indicate that $\hat{x}_2$ can estimate x_2 with satisfactory accuracy. Fig.6 and Fig.7 show the estimation performance of $\hat{x}_3$ for x_3 and the estimation error respectively, which indicate that $\hat{x}_3$ can estimate the total distur

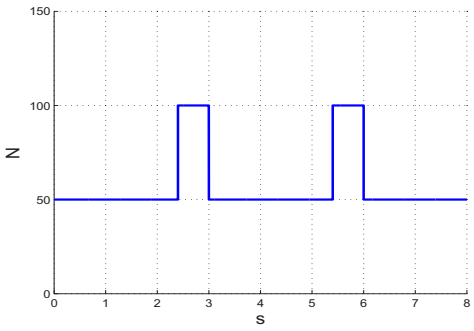

Fig. 1: F_{load}

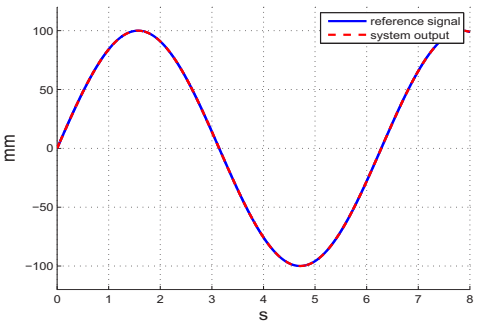

Fig. 2: reference signal and system output

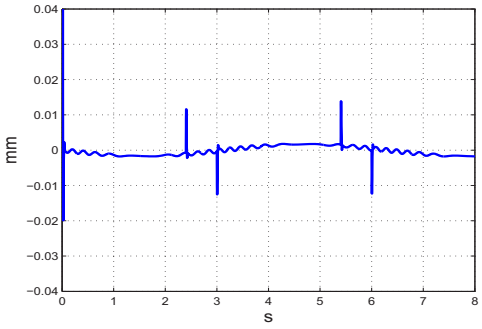

Fig. 3: tracking error

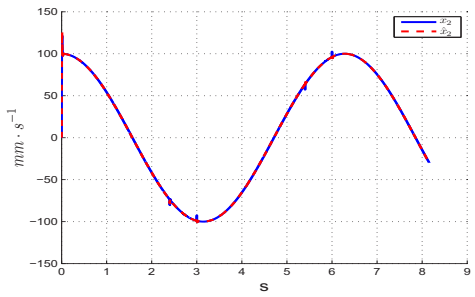

Fig. 4: x_2 and $\hat{x}_2$

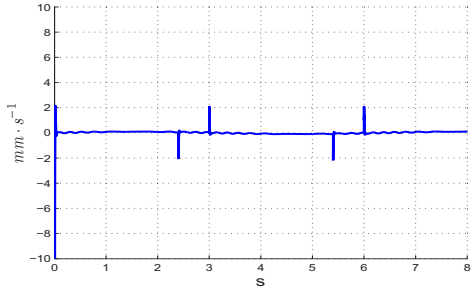

Fig. 5: e_2

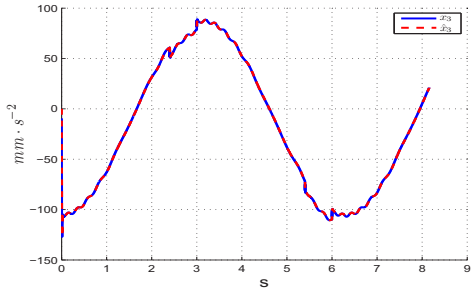

Fig. 6: x_3 and $\hat{x}_3$

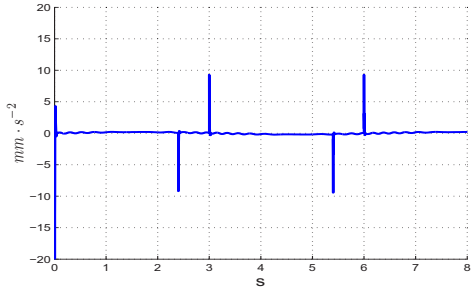

Fig. 7: e_3

6 CONCLUSIONS

In this paper, an ADRC design based on the reduced-order extended state observer(RESO) is proposed for PMLM servo system. Considering the complicated nonlinearity in PMLM including the load force, the friction and the ripple force, the performance of the closed-loop system are analyzed. The relationship between the control precision and the ADRC parameters are discussed. The theoretical analysis and simulation study show that RESO based ADRC can achieve high-precision of PMLM.

References

[1] Brandenburg G, Bruckl S, Dormann J, et al. Comparative investigation of ratary and linear motor feed drive systems for high precision machine tools. The 6th InternationalWorkshop on Advanced Motion Control,2000;384-389.

[2] Guang Feng, Yan-Fei Liu, and Lipei Huang. A New Robust Algorithm to Improve the Dynamic Performance on the Speed Control of Induction Motor Drive. IEEE Transactions On Power Electronics, Vol.19, No.6, November 2004;1624-1627.

[3] J.F.Pan, N.C.Cheung, and J.M.Yang. Auto-disturbance rejection controller for novel planar switched reluctance motor. Proc. Inst. Elect. Eng.łElectr. Power Appl., vol. 153, no. 2, pp. 307C316, Mar. 2006.

[4] Y. X. Su, C. H. Zheng, and B. Y. Duan. Automatic disturbances rejection controller for precise motion control of permanent-magnet synchronous motors. IEEE Trans. Ind. Electron., vol. 52, no. 3, pp. 814C823, Jun. 2005.

[5] Z. G. Liu, S. H. Li. Active Disturbance Rejection Controller Based on Permanent Magnetic Synchronous Motor Model Identification and Compensation. Proceedings of the CSEE. Vol.28 No.24 Aug.25 2008.(In Chinese)

[6] S.Li and Z.Liu. Adaptive speed control for permanent-magnet synchronous motor system with variations of load inertia. IEEE Trans. Ind. Electron., vol. 56, no. 8, pp. 3050C3059, Aug. 2009.

[7] D. Wu, K. Chen, and X. Wang. Tracking control and active disturbance rejection with application to noncircular machining. Int. J. Mach. Tool Manuf., Dec. 2007, vol. 47, no. 15, 2207C2217.

[8] D. Wu, Ken Chen. Design and analysis of precision active disturbance rejection control for noncircular turning process. IEEE Transactions on Industrial Electronics, July 2009, Vol. 56, No. 7, 2746-2753.

[9] Y. Xiao and K. Y. Zhu. Optimal Synchronization Control of High-Precision Motion Systems. IEEE Transactions On Inductrial Electronics, Aug 2006, Vol. 53, No. 4.

[10] K. K. Tan, S. N. Huang, and T. H. Lee. Robust Adaptive Numerical Compensation for Friction and Force Ripple in Permanent-Magnet Linear Motors. IEEE Transactions On Magnetics, Jan 2002, Vol. 38, No. 1.

[11] B. Armstrong-Hlouvry, P. Dupont, and C. C. De Wit. A survey of models, analysis tools and compensation methods for the control of machines with friction. Automatica, 1994, vol. 30, no. 7, 1083C1138.

[12] C. Rohrig and A. Jochheim. Motion control of linear permanent magnet motors with force ripple compensation. American Control Conference, 2001. Proceedings of the 2001, vol. 3, 2001, 2161- 2166.

[13] Jingqing Han. Active disturbance rejection control technique. National Defense Industry Press, Beijing, 2008.(In Chinese).

[14] Yi Huang and Wenge Zhang. Development of active disturbance rejection controller. Control Theory and Application, 19(4):485-492,2002.(In Chinese).

[15] Yi Huang and Jingqing Han. Analysis and design for nonlinear continuous extended state observer. Chinese Bulletin, 45(21):1938-1944,2000.

[16] Yang X, Huang Y. Capability of extended state observer for estimating uncertainties. Proc. of the 2009 American Control Conference, 2009.

[17] Xue W C, Huang Y. The active disturbance rejection control for a class of MIMO block lower-triangular system. Proceedings of the 2011 Chinese Control Conference, 2011.

[18] Xue W C. On Theoretical Analysis of Active Disturbance Rejection Control. Doctoral thesis. Academy of Mathematics and Systems Science, Chinese Academy of Sciences, 2012.